

Supersonic Flow, Part I—Theory and Application,” NASA CR-2228, May 1973, pp. 43–46.

<sup>11</sup>Hess, J.L., “The Use of Higher Order Surface Singularity Distribution to Obtain Improved Potential Flow Solutions for Two-Dimensional Lifting Airfoils,” *Computer Methods in Applied Mechanics and Engineering*, Vol. 5, Jan. 1975, pp. 11–35.

<sup>12</sup>Hess, J.L., “Review of Integral-Equation Techniques for Solving Potential-Flow Problems with Emphasis on the Surface-Source Method,” *Computer Methods in Applied Mechanics and Engineering*, Vol. 5, March 1975, pp. 145–196.

<sup>13</sup>Jacobs, E.N., Ward, K.E., and Pinkerton, R.M., “The Characteristics of 78 Related Airfoil Sections from Tests in the Variable-Density Wind Tunnel,” NACA TR 460, 1933, pp. 299–354.

<sup>14</sup>Raj, P., “A Method of Computing the Potential Flow on Thick Wing Tips,” Ph.D. dissertation, School of Aerospace Engineering, Georgia Institute of Technology, Atlanta, Ga., 1976.

<sup>15</sup>Shen, C.C., Lopez, M.L., and Wasson, N.F., “Jet-Wing Lifting-Surface Theory Using Elementary Vortex Distributions,” *Journal of Aircraft*, Vol. 12, May 1975, pp. 448–456.

<sup>16</sup>Abbott, I.H. and von Doenhoff, A.E., *Theory of Wing Sections*, Dover Publications Inc., New York, 1959, pp. 309–327.

## Minimum On-Axis Noise for a Propeller or Helicopter Rotor

Martin R. Fink\*

United Technologies Research Center,  
East Hartford, Conn.

### Introduction

ONE ultimate noise floor for fixed-wing aircraft is the airframe noise caused by flow of the wing's turbulent boundary layer past the wing trailing edge. A simple method for predicting the spectrum of such noise, using known properties of turbulent boundary layers plus empirical constants, was shown<sup>1</sup> to predict measured flyover noise spectra of aerodynamically clean aircraft such as sailplanes and business jets.

The propeller and hovering helicopter rotor noise radiation which corresponds to airframe noise is broadband noise occurring along the rotational axis. For positions along this axis, the pressure field caused by blade loading and blade thickness is independent of azimuthal position except for fuselage interference effects on loading. Thus the only noise-producing mechanisms are lift fluctuations caused by ingestion of turbulence and airframe noise caused by the blade turbulent boundary layer and vortex wake. Ingestion of atmospheric turbulence was shown<sup>2</sup> to be an important cause of on-axis propeller noise in static operation. This mechanism should be unimportant for helicopter rotors, which have much smaller disc loadings, and becomes less important for propellers as forward speed is increased. There is interest in predicting the ultimate limits on noise from thrusting propulsive devices. Such a prediction method could be obtained from that which had been developed for fixed-wing airframes and evaluated by comparisons with available data.

As shown herein, spectra calculated by a strip-theory equivalent of the method developed for fixed-wing airframe noise generally matched those measured with a thrusting helicopter rotor. They overpredicted the spectra of a non-thrusting propeller, which is a fault caused by overprediction of noise radiation from nonlifting airfoils.

### Prediction Method

An exact equation exists<sup>3</sup> for the noise radiated when one turbulent eddy of known size and intensity is convected past a sharp trailing edge. It was shown<sup>1</sup> that an equation having this analytically derived form, and an empirically determined amplitude, matched available data for peak overall sound pressure level (OASPL) and flyover directivity pattern of aerodynamically clean airframes. This amplitude factor was further adjusted to provide separate predictions of trailing edge noise from the wing and horizontal tail and was given as Eq. (10) of Ref. 1. For an unswept trailing edge, and free-field levels rather than those for a microphone in the presence of ground reflection, this is

$$\begin{aligned} \text{OASPL} = & 50 \log (V/100 \text{ m/s}) + 10 \log (\delta b/R^2) \\ & + 10 \log (\cos \phi \cos \theta/2)^2 + 113.9 \text{ dB} \end{aligned} \quad (1)$$

where  $V$  is the relative velocity and  $\delta$  is the boundary-layer thickness at the trailing edge of the mean geometric chord as calculated for a flat-plate turbulence boundary layer

$$\delta = 0.37 c (Vc/\nu)^{-0.2} \quad (2)$$

Also  $b$  is the span,  $R$  is the far-field distance,  $\phi$  is the sideline angle,  $\theta$  is the direction angle relative to the chord line,  $c$  is the chord, and  $\nu$  is the kinematic viscosity. The free-field 1/3 octave spectrum in the absence of atmospheric attenuation was given by Eq. (7) of Ref. 1

$$\begin{aligned} \text{SPL}_{1/3} - \text{OASPL} = \\ 10 \log \{ 0.613 (f/f_{\max})^4 [(f/f_{\max})^{3/2} + 0.5]^{-4} \} \end{aligned} \quad (3)$$

where  $f_{\max}$ , the frequency at maximum amplitude is given by

$$f_{\max} = 0.1 V/\delta \quad (4)$$

These equations were applied to calculation of noise along the rotational axis of rotating blades. Each blade was regarded as comprised of a large number of radial segments, each with constant relative velocity  $V_T r/r_T$ . Here  $r$  is the average radius at the segment, and the subscript  $T$  denotes the blade tip. Then  $R^2 = X^2 + r^2$  and  $\phi = \cos^{-1} r/X$ , where  $X$  is the distance along the axis of rotation from the blade disc plane to the microphone, and  $\theta$  can be calculated from local blade twist and pitch angle. Span  $b$  of each radial segment should be taken as the product of segment span and number of blades. The spectra calculated for different radial segments can be added to give the complete spectrum.

This calculation method was implemented numerically for the simple case of two constant-chord blades at a great distance (relative to tip radius) from the measurement point. Blade twist and airfoil camber were neglected. Then  $c$ ,  $R$ ,  $\phi$ , and  $\theta$  were independent of radial position, with  $10 \log (\cos \phi \cos \theta/2)^2$  taken equal to  $-3$  dB.

Calculations were conducted of noise on the rotational axis two diameters from a two-blade propeller with 3.05-m diameter and 0.424-m chord, at 136 m/s tip speed. Inboard radial extent of the blade was varied to permit examination of noise contributed by different radial regions. These spectra are plotted in Fig. 1. The outer 10% of the blade is predicted to radiate more than half the noise (within 3 dB of the total) at frequencies above that for peak amplitude. Except for frequencies more than three octaves below the peak-amplitude frequency, essentially all the broadband noise is predicted to come from the region beyond 60% of the tip radius.

### Comparisons with Data

Spectra are available<sup>4</sup> for an unusual propeller with the dimensions assumed above. This propeller had 0.045 rad (2.57

Received June 13, 1978. Copyright © American Institute of Aeronautics and Astronautics, Inc., 1978. All rights reserved.

Index categories: Noise; Propeller and Rotor Systems; Aeroacoustics.

\*Senior Consulting Engineer, Aerodynamics. Associate Fellow AIAA.

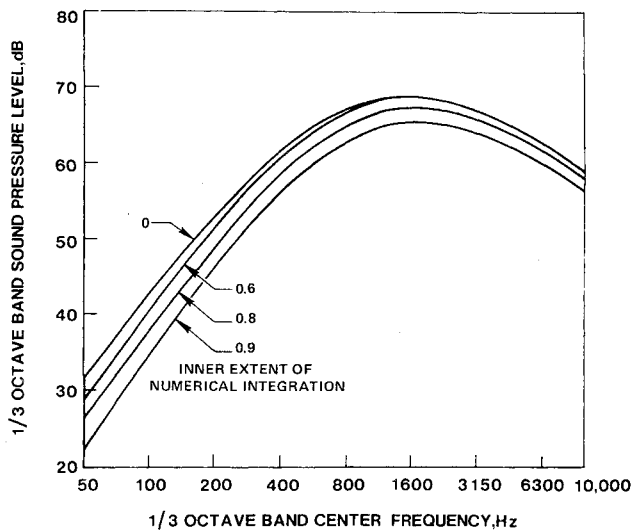


Fig. 1 Effect of blade inner radial extent on calculated 1/3 octave spectrum.

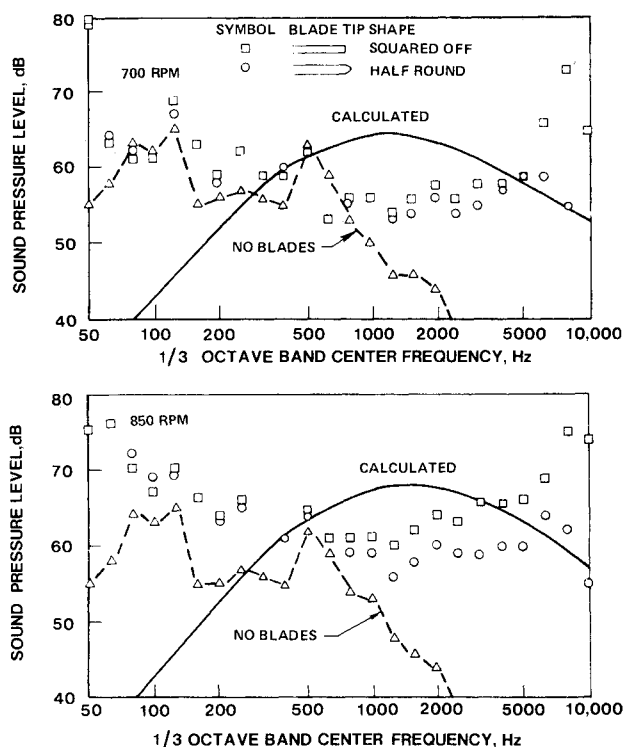


Fig. 2 Measured and calculated 1/3 octave spectra for a non-thrusting propeller.

deg) helical twist and uncambered NACA 0012 airfoil sections, and was operated at airspeeds 0.045 times the rotational tip speed. All radial positions of the blades therefore operated at zero incidence and zero lift, and the turbulent wake shed by each blade was blown downstream of the next blade. Data were measured on the rotation axis two diameters upstream of the hub.

Calculated and measured 1/3 octave spectra on the rotation axis are compared in Fig. 2 for the two highest test speeds. Data for the two tip shapes are plotted herein as square and circle symbols for the squared-off and half-round tips, respectively. Also plotted as triangle symbols are measurements of background noise produced by the wind tunnel and the blade-rotation drive system without the blades. There was little effect of tip shape on noise radiation except at the highest frequencies, where the squared-off tip generated a

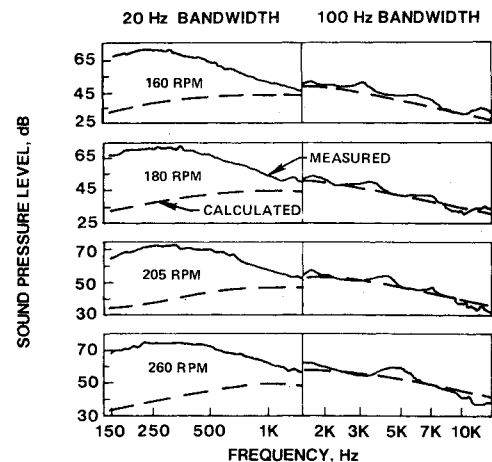


Fig. 3 Measured and calculated constant bandwidth spectra for a helicopter rotor.

sharply peaked spectrum 10 to 20 dB above that for the half-round tip. Measured spectra clearly did not match that calculated for trailing edge noise. Up to 0.5 kHz, the measured spectra were dominated by noise from the wind tunnel and test rig. From 1 to 4 kHz they were approximately constant at levels roughly 8 dB below the calculated peak amplitude. Above 4 kHz, data for the blades with half-round tips generally matched the prediction. Data for lower tip speeds (not shown) were in closer agreement with calculated spectra. This agreement is coincidental because the rig and tunnel background noise, not measured at those conditions, probably set the measured spectrum levels near the calculated peak amplitude.

Fixed-wing flyover data on which the prediction method was based were obtained at moderate lift coefficients, but these rotating-blade data were taken at zero lift. Trailing edge noise spectra for a 0.23-m chord nonrotating NACA 0012 airfoil model at 0- and 6-deg angle-of-attack have been measured<sup>5</sup> in an acoustic wind tunnel by use of a directional microphone. Those data had been compared with spectra calculated by the method<sup>1</sup> used here. Measured spectra for nonzero angle-of-attack were predicted within 3 dB over the indicated frequency range. However, spectra measured at zero lift were overpredicted 5 to 10 dB near the calculated peak-amplitude frequency but were closely predicted above roughly four times that frequency. The comparison<sup>5</sup> between measured and predicted spectrum shapes for a nonlifting nonrotating wing generally matched that shown herein for nonlifting rotating blades. Thus the discrepancy is caused by inadequacy of this simple noise prediction method at zero lift and should not occur for the practical case of thrusting propeller blades.

Spectra were measured at Westland Helicopters<sup>6</sup> with two blades of a full-scale 17-m-diameter Sikorsky S-55 helicopter main rotor. The rotor was mounted inverted on its test stand to prevent ingestion of the turbulent wake. Such ingestion could increase the measured noise. A microphone was located 75 deg above the rotor plane (15 deg from the rotation axis) at 76 m from the hub, out of the rotor wake. Constant bandwidth spectra at this position were given for four rotation speeds. Rotor thrust had been held constant as rotation speed was varied. These spectra are compared in Fig. 3 with those calculated by the method described herein, converted from 1/3 octave to constant bandwidth. The portion of these data below 1.5-kHz center frequency is caused by other noise-generating processes. The high-frequency portion contains a narrow hump of broadband noise which shifts from about 3 kHz at the lowest rotation speed to about 5 kHz at the highest. This linear variation of frequency with rotation speed matches the behavior of the blade tip noise shown in Fig. 2. Peak amplitude of this hump was several dB above the calculated

spectra. The remaining portion of the measured broadband spectrum above 1.5-kHz center frequency was closely predicted. Thus the helicopter rotor noise called<sup>6</sup> high-frequency broadband noise is attributed to flow of the blade turbulent boundary layer past the trailing edge. It is adequately predicted by a method developed for calculating such noise from fixed-wing aircraft, applied to local conditions at all radial stations on a rotating blade.

### Conclusions

1) Predicted on-axis broadband noise caused by flow of the blade turbulent boundary layer past the trailing edge generally matches the portion of a hovering helicopter rotor's spectrum called high-frequency broadband noise.

2) Noise radiation from nonlifting blades with their shed wakes blown downstream is overestimated near peak amplitude by this method. The same overestimate occurs when predictions by the fixed-wing version of this method are compared with data for nonlifting airfoils. Good agreement occurs at sufficiently higher frequencies for both nonrotating and rotating blades.

### References

- <sup>1</sup>Fink, M.R., "Airframe Noise Prediction Method," FAA-RD-77-29, March 1977.
- <sup>2</sup>Hanson, D.B., "A Study of Subsonic Fan Noise Sources," *Progress in Astronautics and Aeronautics*, Vol. 44, edited by I.R. Schwartz, AIAA, New York, 1976, pp. 209-232.
- <sup>3</sup>Ffowcs-Williams, J. and Hall, L.H., "Aerodynamic Sound Generation by Turbulent Flow in the Vicinity of a Scattering Half Plane," *Journal of Fluid Mechanics*, Vol. 40, March 1970, pp. 657-670.
- <sup>4</sup>Scheiman, J., Hilton, D.A., and Shivers, J.P., "Acoustical Measurements of the Vortex Noise for a Rotating Blade Operating With and Without Its Shed Wake Blown Downstream," NASA TN D-6364, Aug. 1971.
- <sup>5</sup>Schlinder, R.H., "Trailing Edge Noise Measurements With a Directional Microphone," AIAA Paper 77-1269, 4th Aeroacoustics Conference, Atlanta, Ga., Oct. 1977.
- <sup>6</sup>Leverton, J.W. and Pollard, J.S., "A Comparison of the Overall and Broadband Noise Characteristics of Full-Scale and Model Helicopter Rotors," *Journal of Sound and Vibration*, Vol. 30, Sept. 1973, pp. 135-152.

## Compressibility Effects on Parachute Transient Pressures

Paul C. Klimas\*

Sandia Laboratories, Albuquerque, N. Mex.

### Introduction

**D**URING inflation of a parachute the peak unsteady differential pressures are greater than corresponding steady values. These transient loadings should ideally be used for canopy structural design, but this is not normally done because the task of analytically describing the unsteady, viscous, often compressible airflow about a flexible, porous structure is a difficult one. Experimentally, the large number of variables (Mach and Reynolds number, canopy geometry, canopy materials, dynamic pressure, mass ratios, etc.) involved in inflation dynamics make it economically unfeasible to run a comprehensive descriptive test program. As a result, most designers account for dynamic effects through design factors determined by trial and error.

Received July 11, 1978. Copyright © American Institute of Aeronautics and Astronautics, Inc., 1978. All rights reserved.

Index categories: Nonsteady Aerodynamics; Deceleration Systems.

\*Member of Technical Staff, Aerodynamics Department 1330. Member AIAA.

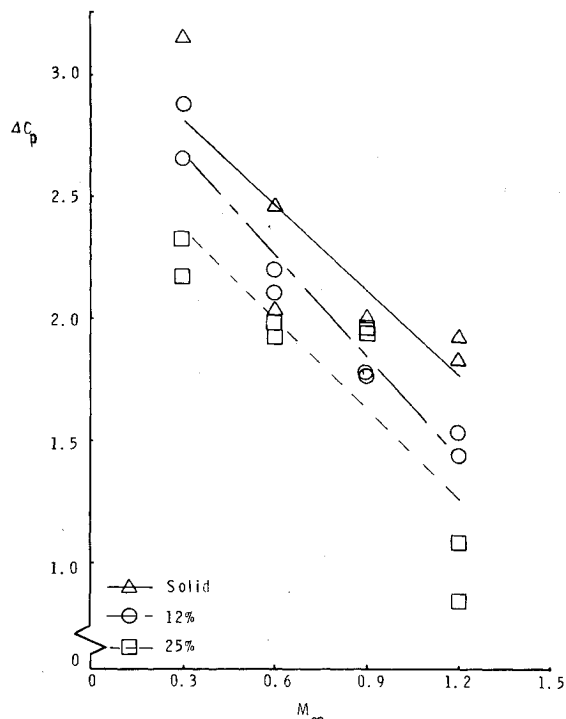


Fig. 1 Transient differential pressure coefficients,  $l/r = 0.95$ .

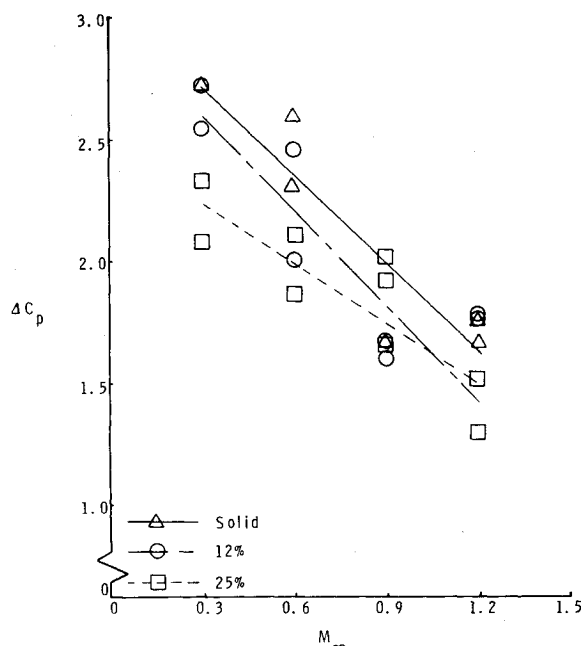


Fig. 2 Transient differential pressure coefficients,  $l/r = 0.82$ .

Even with the above cited obstacles, two very interesting publications in this subject area have appeared. Melzig and Schmidt<sup>1</sup> measured unsteady pressures on inflating canopies at low subsonic Mach numbers. When expressed in differential pressure coefficient form ( $\Delta C_p \equiv (p_{in} - p_{out})/q_\infty$ ), the maximum unsteady values were often many times the steady values. The multiplier increased as freestream velocity decreased. This qualitative trend was predicted analytically by Eldred and Mikulas<sup>2</sup> through the one-dimensional, unsteady gasdynamical equations. Their formulation showed  $\Delta C_p$  to be inversely proportional to freestream Mach number. The present work attempts to both expand the available information in this area and isolate the dependence of transient aerodynamics on freestream Mach number. This is done by examining parachutes of three different geometric porosities